Journal of the Serbian Chemical Society
JSCS@tmf.bg.ac.rs • www.shd.org.rs/JSCS
J. Serb. Chem. Soc. *87* (2) S38–S46 (2022) *Supplementary material*

SUPPLEMENTARY MATERIAL TO

Evaluation of antitumor potential of Cu(II) complex with hydrazone of 2-acetylthiazole and Girard's T reagent

NEVENA STEVANOVIĆ[1], MIMA JEVTOVIĆ[2], DRAGANA MITIĆ[2], IVANA Z. MATIĆ[3], MARIJA ĐORĐIĆ CRNOGORAC[3], MIROSLAVA VUJČIĆ[4], DUŠAN SLADIĆ[1], BOŽIDAR ČOBELJIĆ[1] and KATARINA ANĐELKOVIĆ[1]*

[1]University of Belgrade-Faculty of Chemistry, Studentski trg 12–16, 11000 Belgrade, Serbia,[2]Innovative centre of the Faculty of Chemistry, Studentski trg 12–16, 11000 Belgrade, Serbia, [3]Institute of Oncology and Radiology of Serbia, 11000 Belgrade, Serbia and [4]University of Belgrade-Institute of Chemistry, Technology and Metallurgy, Department of Chemistry, Njegoševa 12, 11000 Belgrade, Serbia

J. Serb. Chem. Soc. *87* (2) (2022) 181–192

SPECTROSCOPIC DATA OF SYNTHESIZED COMPOUNDS

*Ligand **HL**Cl*

IR (ATR): 3387w, 3128w, 3091m, 3017m, 2955s, 1701vs, 1612w, 1550vs, 1486s, 1401m, 1300w, 1201s, 1135w, 976w, 944w, 914m, 786w, 748w, 684w, 585w, 551w. (**HL**[1]Cl -*E*). ^{1}H NMR (500 MHz, DMSO-d_6, δ): 2.41 (*s*, 3H, H-5), 3.30 (*s*, 9H, H-8), 4.60 (*s*, 2H, H-7), 7.85 (*d*, 1H, *J* = 5.0, H-2), 7.93 (*d*, 1H, *J* = 5.0, H-3), 11.61 (*s*, 1H, N-H). ^{13}C NMR (125 MHz, DMSO-d_6, δ): 13.90 (C-5), 53.65 (C-8), 63.01 (C-7), 123.33 (C-2), 143.94 (C-3), 146.98 (C-4), 161.23 (C-1), 167.04 (C-6). (**HL**[1]Cl -*Z*). ^{1}H NMR (500 MHz, DMSO-d_6, δ): 2.53 (*s*, 3H, H-5), 3.34 (*s*, 9H, H-8), 4.82 (*s*, 2H, H-7), 7.85 (*d*, 1H, *J* = 5.0, H-2), 7.93 (*d*, 1H, *J* = 5.0, H-3), 11.86 (*s*, 1H, N-H).^{13}C NMR (125 MHz, DMSO-d_6, δ), : 15.05 (C-5), 53.89 (C-8), 63.76 (C-7), 123.65 (C-2), 143.97 (C-3), 150.80 (C-4), 166.78 (C-1), 167.34 (C-6).

*The Cu(II) complex **1***

Yield: 42 mg (36 %). Combustion analysis for $C_{11}H_{20}BCuF_4N_7O_2S$: Calculated. C 28.43, H 4.34, N 21.10, S 6.90; found C 28.53, H 4.15, N 21.17, S 6.89. IR (ATR): 3352w, 3317w, 3077m, 3050s, 2970m, 2940w, 2047vs, 1829w, 1698w, 1604w, 1522s, 1477m, 1444m, 1413m, 1395m, 1325m, 1287m, 1239w, 1159w, 1124w, 1088w, 1053m, 1007m, 961w, 939w, 917m, 878w, 783m, 735w, 656w, 631w, 563w.

* Corresponding author. E-mail: kka@chem.bg.ac.rs

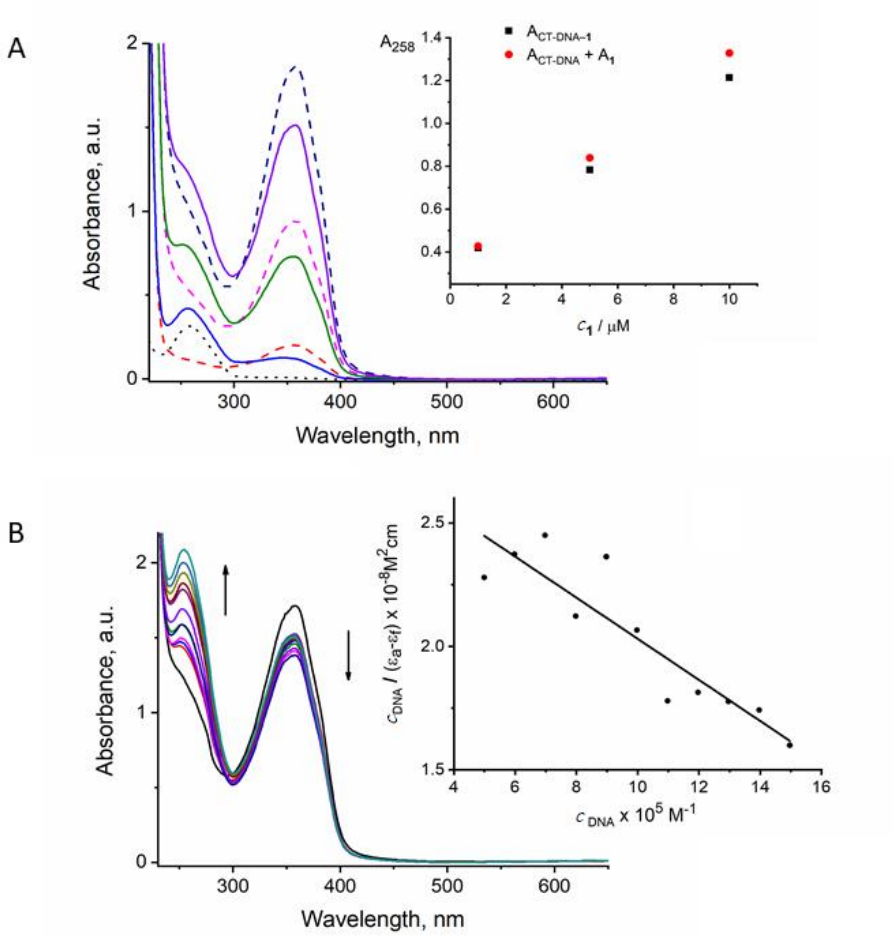

Fig. S-1. DNA-binding activity: (A) UV–Vis absorption spectra of CT-DNA (49.9 μM, dotted line), complex **1** (1, 5, and 10 μM, dashed lines) and **1**–CT-DNA after the interaction (solid lines); in the inset comparison of absorption at 258 nm between the CT-DNA–**1** and the sum of the values of CT-DNA and **1**; (B) – The absorbance titration of the compound **1** (10 μM) by gradually increasing the concentration of double stranded CT-DNA (4.99, 5.98, 6.98, 7.98, 8.98, 9.98, 10.98, 11.97, 12.97, 13,97 and 14.97 × 10^{-5} M); the arrows show the changes in absorbance with increasing amounts of CT-DNA; in the inset is shown the plot of $c_{DNA}/(\varepsilon_A - \varepsilon_F)$ *versus* c_{DNA}.

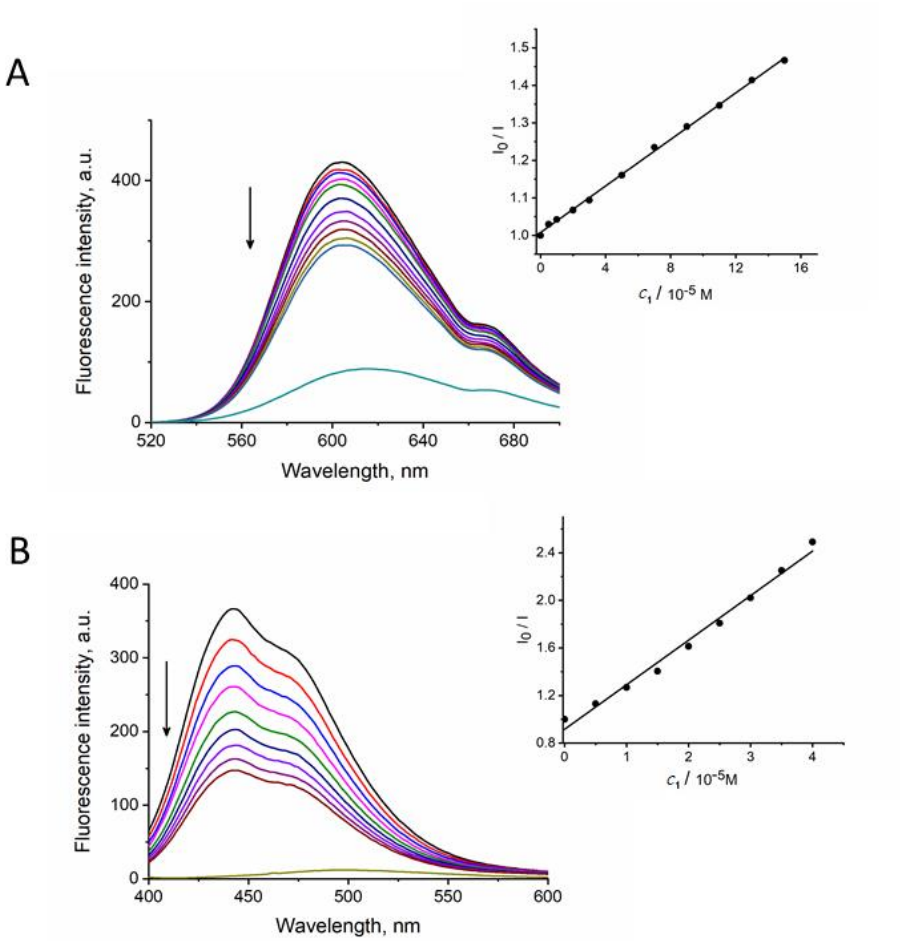

Fig. S-2. Fluorescence displacement study: (A) – changes in emission spectra of ethidium bromide (2.5×10^{-5} M) bound to CT-DNA (9.7×10^{-5} M) and quenching of EB–CT-DNA system by increasing concentrations of **1** (B) – Changes in emission spectra of Hoechst 33258 (2.8×10^{-5} M) bound to CT-DNA (9.7×10^{-5} M) and quenching H–CT-DNA system by increasing concentrations of **1**. The arrows show that fluorescence intensity decreased with increasing concentration of the complex. The insets in panels (A) and (B) show fluorescence quenching curves of EB bound to DNA at λ_{max} = 600 nm by **1**, and H bound to DNA at λ_{max} = 443 nm by **1**, respectively.

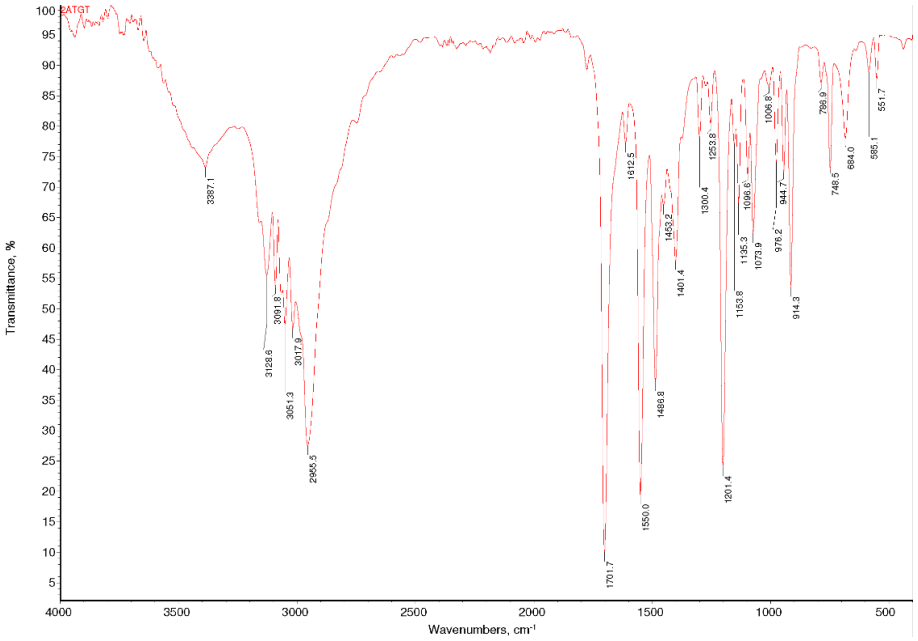

Fig. S-3. IR spectra of ligand **HL**Cl

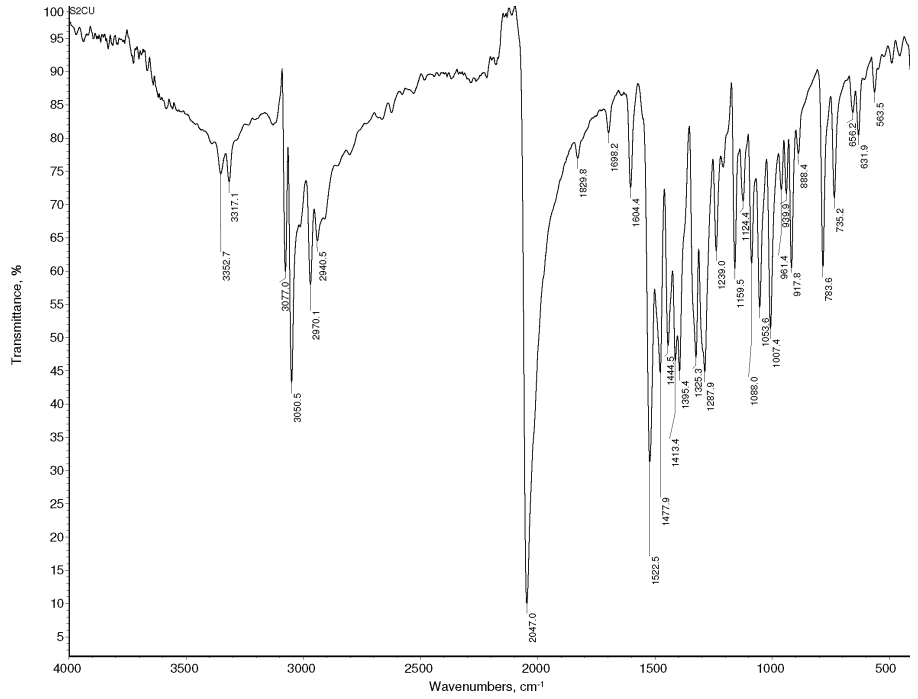

Fig. S-4. IR spectra of complex **1**

BIOLOGICAL ACTIVITY

Measurement of intracellular reactive oxygen species (ROS) levels in HeLa and HaCaT cell lines

HeLa cells were incubated with IC_{50} concentration of Cu(II) complex for 24 h. After the incubation, the cells were collected by trypsinnization, washed with PBS and incubated again in a solution of 30 μM 2′,7′-dichlorodihydrofluorescein diacetate in PBS for 45 min at 37 °C, according to the previously described procedure.[1] The cells were then washed with PBS and intracellular ROS levels were assessed by flow cytometry.

HaCaT cells were incubated with subtoxic IC_{20} concentration of Cu(II) complex for 24 h (applied concentration was 20 μM, as assessed by MTT test for 24 h treatment). Afterwards, the cells were collected, washed and incubated in a solution of 30 μM 2′,7′-dichlorodihydrofluorescein diacetate in PBS for 45 min at 37 °C. After the incubation and washing, the cell samples were exposed to 4 mM hydrogen peroxide solution (H_2O_2) to induce the generation of ROS for 30 min at 37 °C. After 30 min, these cells were washed with PBS and analyzed.

The intensity of green fluorescence emitted by dichlorofluoresceinin in HeLa and HaCaT cells was measured by flow cytometry. Data are presented as mean ± S.D. of two independent experiments.

Effects of Cu(II) complex on intracellular ROS levels

In order to explore the possible role of ROS generation in mediating cytotoxic effects of novel Cu(II) complex (**1**), the intracellular ROS level in HeLa cells treated with IC_{50} concentration of the complex for 24 h was measured by flow cytometry using 2′,7′-dichlorodihydrofluorescein diacetate as a fluorescent probe. The effects of the complex on intracellular ROS levels in HeLa cells are presented in Fig. S-5. The tested Cu(II) complex **1** remarkably decreased the intracellular ROS level in HeLa cells, when compared with basal intracellular ROS level in untreated control cell samples, suggesting the antioxidant properties of tested complex at lower sub-toxic concentration.

Due to potential radical-scavenging activity of the novel complex, applied at subtoxic concentration, the effect of the complex on generation of intracellular ROS induced by H_2O_2 in normal keratinocytes HaCaT was examined, as it can be seen in Fig. S-6. Preincubation of normal HaCaT cells with subtoxic IC_{20} concentration of the complex for 24 h induced an increase in the intracellular ROS level triggered by exogenously added H_2O_2, in comparison with this level in untreated control cells exposed only to H_2O_2, pointing to prooxidant activity of **1** in the presence of H_2O_2 in normal cells. This is in accordance with the studies reporting an increase in intracellular ROS production induced by some copper complexes.[2-4] Therefore, it is possible that higher toxic concentrations of

the investigated Cu(II) complex **1** may modulate differently intracellular ROS levels in cancer cells.

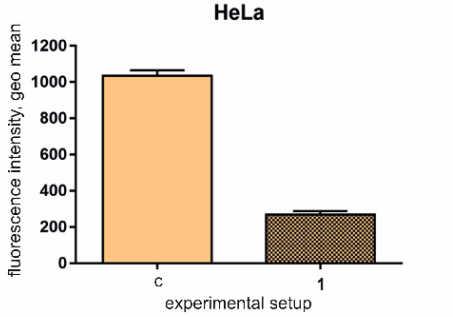

Fig. S-5. Effects of 24 h pretreatment of HeLa cells with IC_{50} concentration of the Cu(II) complex (**1**) on intracellular ROS level.

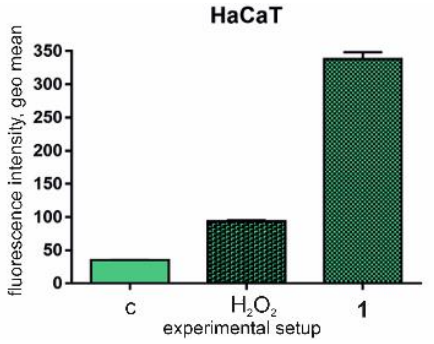

Fig. S-6. Effects of 24 h pretreatment of HaCaT cells with IC_{20} concentration of Cu(II) complex **1** on intracellular ROS production induced by hydrogen peroxide.

BSA fluorescence measurements

For BSA fluorescence measurements, BSA concentration in 40 mM bicarbonate buffer was kept constant in all samples, while the concentration of the compounds was increased: into 1 mL of buffer 10 μL of stock solution of BSA (1 mg/mL) and 0.5 μL of stock solution of the compound (10 mM) were added and incubated for 10 min. The emission spectra in range 295 to 500 nm were recorded (excitation wavelength 280 nm). Another 0.5 μL of the solution of **1** was successively added at final concentrations of **1**: 5×10^{-6} M, 1, 1.5, 2, 2.5. 3, 3.5, 4, 4.5, 5, 5.5 and 6×10^{-5} M. The change in the fluorescence intensity was measured.

BSA interaction studies

BSA has often been used as a model protein to measure the albumin-binding ability of drugs and metal complexes. Fig. S-7 shows that BSA exhibited an

intense fluorescence emission band at 335 nm when excited at 296 nm, due to presence of tryptophan residues Trp-134 and Trp-212.[5] The addition of increasing concentrations of **1** to BSA solution resulted in a significant quenching of fluorescence intensity, indicating the interaction of the complex with the protein. The obtained strong decrease in fluorescence intensity at maximum wavelength (by 65 %) and a blue shift (about 14 nm) suggested that the complex caused significant conformational changes in the secondary structure of albumin. The fluorescence quenching data were further analyzed with the Stern-Volmer equation (S-1).[6]

$$I_0/I = 1 + K_q\tau_0 c_Q = 1 + K_{sv}c_Q \quad \text{(S-1)}$$

$$K_q = K_{sv} / \tau_0 \quad \text{(S-2)}$$

where I and I_0 are the steady state fluorescence intensities in presence and absence of a quencher, respectively. K_{sv} is the Stern-Volmer constant and c_Q is concentration of the quencher; τ_0 is the average lifetime of the protein without the quencher. As shown in insets in Fig. S-7, good linear fitting linearity of the plot suggests that the Stern-Volmer model is appropriate for studying the binding mechanism between **1** and BSA. The Stern-Volmer constant K_{sv} and the quenching constant K_q were calculated using the equations (S-1) and (S-2), respectively. K_{sv} for **1** was calculated from the plot of I_0/I versus c_1 as 2.75×10^4 M^{-1}. Assuming that average lifetime of the biomolecule is around 10^{-8} s^{-1} [7] K_q value for **1** was calculated to be 2.75×10^{-12} $M^{-1}s^{-1}$, indicating static quenching, *i.e*. the formation of a nonfluorescent complex between the compound and BSA.

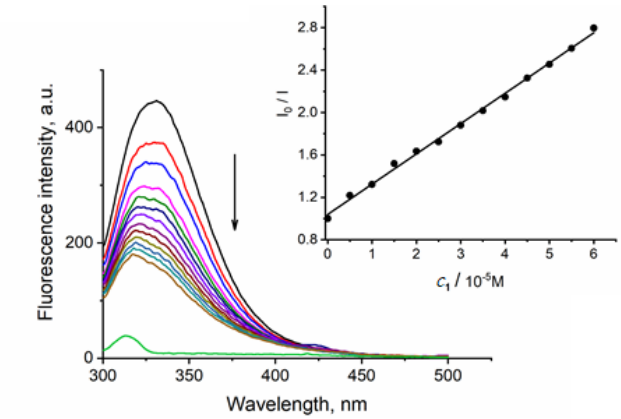

Fig. S-7. Fluorescence spectra of BSA in the absence and presence of increasing concentrations of **1**. Value of K_{sv} was calculated from the plot I_0/I versus c_1 shown in inset. The arrow shows the decrease in fluorescence intensities with increasing concentrations of the complex.

DNA cleavage experiments. For DNA cleavage experiments, plasmid pUC19 (pUC19, 2686 bp, purchased from Sigma-Aldrich, USA) was prepared by its

transformation in chemically competent cells *Escherichia coli* strain XL1 blue. Amplification of the clone was done according to the protocol for growing *E. coli* culture overnight in LB medium at 37 ºC[8] and purification was performed using Qiagen Plasmid plus Maxi kit. Finally, DNA was eluted in 10 mM Tris-HCl buffer and stored at –20 ºC. The concentration of plasmid DNA (550 ng/μL) was determined by measuring the absorbance of the DNA-containing solution at 260 nm. One optical unit corresponds to 50 μg/mL of double stranded DNA.

The cleavage reaction of supercoiled pUC19 DNA (550 ng) with complex **1** (1, 2, 3, 4, 5, 6 and 7 mM) was performed in a 20 μL reaction mixture in 40 mM bicarbonate buffer pH 8.4 at 37 ºC, for 90 minutes. The reaction mixtures were vortexed from time to time. The reaction was terminated by short centrifugation at 10000 rpm and addition of 5 μL of loading buffer (0.25 % bromophenol blue, 0.25 % xylene cyanol FF and 30 % glycerol in TAE buffer, pH 8.24 (40 mM Tris-acetate, 1 mM EDTA)). The samples were subjected to electrophoresis on 1 % agarose gel (Amersham Pharmacia-Biotech, Inc) prepared in TAE buffer pH 8.24. The electrophoresis was performed at a constant voltage (80 V) until bromophenol blue had passed through 75 % of the gel. A Submarine Mini-gel Electrophoresis Unit (Hoeffer HE 33) with an EPS 300 power supply was used. After electrophoresis, the gel was stained for 30 min by soaking it in an aqueous ethidium bromide solution (0.5 μg/mL). The stained gel was illuminated under a UV transilluminator Vilber-Lourmat (France) at 312 nm and photographed with a Nikon Coolpix P340 Digital Camera through filter DEEP YELLOW 15 (TIFFEN, USA).

DNA cleavage. The type of DNA interactions with the metal complex has been further established by the investigation of damage to circular DNA. The nuclease efficiency of the Cu(II) complexes is usually investigated using different activators for initiating the DNA cleavage.[9] In this work, the ability of **1** to cleave double-stranded plasmid DNA in the absence of reducing agents was investigated using an agarose electrophoretic assay by monitoring the conversion of supercoiled form (FI) plasmid DNA into the nicked (FII) and the linear form (FIII). As shown in Fig. S-8 (lane 1), plasmid pUC19 consisted mainly of FI and FII. Upon the addition of an increasing concentration of complex **1** to the plasmid, a gradual diminishing of the amount of supercoiled form FI, followed by the formation of nicked form FII, occurred. In addition, the bands corresponding to FI and FII forms smeared at a much higher concentration of **1** (5, 6 and 7 mM, lanes 6, 7 and 8, respectively), indicating the nuclease activity of the complex, which converts DNA to shorter fragments. The form FIII was not observed at the applied concentration range of **1**, indicating that the double strand scission did not occur upon the interaction of complex Cu(II) with circular DNA.

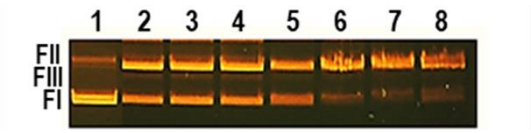

Fig. S-8. DNA cleavage activity of **1**: the agarose gel electrophoretic pattern of supercoiled form FI, open form FII and linear form FIII of pUC19 (0.32 μM; lane 1) after an interaction with **1** (1, 2, 3, 4, 5, 6 and 7 mM, lanes 2–8, respectively).

REFERENCES

1. N. Mihailović, V. Marković, I. Z. Matić, N. S. Stanisavljević, Ž. S. Jovanović, S. Trifunović, L. Joksović, *RSC Advances* **7** (2017) 8550 (http://dx.doi.org/10.1039/C6RA28787E)
2. C. R. Kowol, P. Heffeter, W. Miklos, L. Gille, R. Trondl, L. Cappellacci, W. Berger, B. K. Keppler, *J. Biol. Inorg. Chem.* **17** (2012) 409 (http://dx.doi.org/10.1007/s00775-011-0864-x)
3. A. Sîrbu, O. Palamarciuc, M. v. Babak, J. M. Lim, K. Ohui, E. A. Enyedy, S. Shova, D. Darvasiová, P. Rapta, W. H. Ang, V. B. Arion, *Dalton Trans.* **46** (2017) 3833 (http://dx.doi.org/10.1039/C7DT00283A)
4. C. Shobha Devi, B. Thulasiram, R. R. Aerva, P. Nagababu, *J. Fluoresc.* **28** (2018) 1195 (http://dx.doi.org/10.1007/s10895-018-2283-7)
5. C. Protogeraki, E. G. Andreadou, F. Perdih, I. Turel, A. A. Pantazaki, G. Psomas, *Eur. J. Med. Chem.* **86** (2014) 189 (http://dx.doi.org/10.1016/j.ejmech.2014.08.043)
6. K. Ghosh, S. Rathi, D. Arora, *J. Lumin.* **175** (2016) 135 (http://dx.doi.org/10.1016/j.jlumin.2016.01.029)
7. P. Banerjee, S. Pramanik, A. Sarkar, S. C. Bhattacharya, *J. Phys. Chem. B* **113** (2009) 11429 (http://dx.doi.org/10.1021/jp811479r)
8. W. J. Dower, J. F. Miller, C. W. Ragsdale, *Nucleic Acids Res.* **16** (1988) 6127 (http://dx.doi.org/10.1093/nar/16.13.6127)
9. K. Ghosh, P. Kumar, N. Tyagi, U. P. Singh, V. Aggarwal, M. C. Baratto, *Eur. J. Med. Chem.* **45** (2010) 3770 (http://dx.doi.org/10.1016/j.ejmech.2010.05.026).